

The Starting Material Concentration Dependence of Ag_3PO_4 Synthesis for Rhodamine B Photodegradation under Visible Light Irradiation

Febiyanto and Uyi Sulaeman*

Department of Chemistry Faculty of Mathematics and Natural Sciences Universitas Jenderal Soedirman
Jl. Dr. Soeparno No. 61 Karangwangkal Purwokerto Central Java Indonesia 53123

*Corresponding author: uyi_sulaeman@yahoo.com

Received: February 2020; Revision: March 2020; Accepted: April 2020; Available online: May 2020

Abstract

Synthesis of Ag_3PO_4 photocatalyst under the varied concentrations of AgNO_3 and $\text{Na}_2\text{HPO}_4 \cdot 12\text{H}_2\text{O}$ as starting material has been successfully synthesized using the co-precipitation method. The concentration of AgNO_3 is 0.1; 0.5; 1.0; and 2.0 M, whereas $\text{Na}_2\text{HPO}_4 \cdot 12\text{H}_2\text{O}$ is 0.03; 0.17; 0.33; and 0.67 M, respectively. The co-precipitations were carried out under aqueous solution. As-synthesized photocatalysts were examined to degrade Rhodamine B (RhB) under blue light irradiation. The results showed that varying concentrations of starting materials affect the photocatalytic activities, the intensity ratio of [110]/[200] facet plane, and their bandgap energies of Ag_3PO_4 photocatalyst. The highest photocatalytic activity of the sample was obtained by synthesized using the 1.0 M of AgNO_3 and 0.33 M of $\text{Na}_2\text{HPO}_4 \cdot 12\text{H}_2\text{O}$ (AP-1.0). This is due to the high [110] facet plane and increased absorption along the visible region of AP-1.0 photocatalyst. Therefore, this result could be a consideration for the improvement of Ag_3PO_4 photocatalyst.

Keywords: Ag_3PO_4 , co-precipitation method, photocatalytic activity, Rhodamine B.

DOI: 10.15408/jkv.v6i1.14837

1. INTRODUCTION

To date, silver orthophosphate or Ag_3PO_4 photocatalyst has been promising visible light-activated photocatalyst material. This because of their small bandgap energy (~2.40 eV) and their quantum efficiency of nearly ~90% under visible light or above 520 nm (Yi *et al.*, 2010). In addition, it has greater photocatalytic efficiency than well-known traditional photocatalyst like doped- TiO_2 (Katsumata *et al.*, 2013), TiO_2 commercial (P25) (Liu *et al.*, 2012), and ZnO (Khan *et al.*, 2012).

To enhancing their photocatalytic activities, some modifications have been prepared and investigated. They were doping (Song *et al.*, 2017; Xie and Wang, 2014; Yu *et al.*, 2015), composite fabrication (Chen *et al.*, 2013; Zhankui *et al.*, 2013) and morphology design (Dong *et al.*, 2014; Guo *et al.*, 2015; Sulaeman *et al.*, 2016; Vu *et al.*, 2013). The modifications were also carried out by using the addition of complex solution (Wang *et al.*, 2012; Xu and Zhang, 2013), the hydrophilic

polymer (Yang *et al.*, 2014), various reactant composition (Bozetine *et al.*, 2013), stirring time (Yan *et al.*, 2013) and temperature (Wang *et al.*, 2015). These modifications showed a significant effect on the photocatalytic activities of Ag_3PO_4 photocatalyst.

Recently, the different morphology, particle size, crystallinity, and absorption profiles could be resulted in the different concentrations of KH_2PO_4 as starting material in the Ag_3PO_4 synthesis. This might be due to the different concentration influenced the nucleation and crystal growth during photocatalyst synthesis. However, the high photocatalytic activity of Ag_3PO_4 photocatalyst can be found in the sample with smaller particle size, higher crystallinity, and UV-Vis absorption ability of Ag_3PO_4 (Afifah *et al.*, 2019). Besides KH_2PO_4 , the reactant of $\text{Na}_2\text{HPO}_4 \cdot 12\text{H}_2\text{O}$ as a source of phosphate has been applied for Ag_3PO_4 design synthesis (Chen, Dai, Guo, Bu, & Wang, 2016; Wang *et al.*, 2015; Wu *et al.*, 2013). Nevertheless, the investigation using the variation of

$\text{Na}_2\text{HPO}_4 \cdot 12\text{H}_2\text{O}$ concentration has not been reported. Based on these reports, it is a good idea to obtain high photocatalytic activity by using $\text{Na}_2\text{HPO}_4 \cdot 12\text{H}_2\text{O}$. Therefore, we have tried to observe the effect of the varied concentration of AgNO_3 and $\text{Na}_2\text{HPO}_4 \cdot 12\text{H}_2\text{O}$ as starting material for Ag_3PO_4 co-precipitation. The activities of the products were investigated using the Rhodamine B (RhB) photodecomposition under blue light irradiation.

2. MATERIALS AND METHODS

Materials

Materials were used without further purification, such as a commercial textile dye of RhB, distilled water (DW), AgNO_3 (Merck), and $\text{Na}_2\text{HPO}_4 \cdot 12\text{H}_2\text{O}$ (Merck).

Photocatalyst Characterization

Determination of crystallinity and purity of samples was done using X-ray diffraction (XRD) Bruker AXS D2 Phaser. UV and visible light absorption profiles were conducted using Diffuse Reflectance Spectroscopy (DRS) JASCO V-670. Photocatalyst samples were examined under blue light irradiation of LED Skyled (3W/220V) for RhB photodegradation. Lamp-suspension surface distance was adjusted at 10 cm. The absorbance of filtrate after the photodegradation process was analyzed using UV-Visible spectroscopy Shimadzu 1800.

Synthesis of Ag_3PO_4 Photocatalyst with The Varied Concentration of Reactants

Photocatalyst was synthesized using the co-precipitation method by reacting AgNO_3 and $\text{Na}_2\text{HPO}_4 \cdot 12\text{H}_2\text{O}$ with various concentrations of reactants. The concentration of $\text{Na}_2\text{HPO}_4 \cdot 12\text{H}_2\text{O}$ was 0.03, 0.17, 0.33, and 0.67 M were slowly mixed drop by drop in room temperature into 0.1, 0.5, 1.0, and 2.0 M of AgNO_3 , respectively. The reactants of AgNO_3 and $\text{Na}_2\text{HPO}_4 \cdot 12\text{H}_2\text{O}$ were stoichiometrically synthesized following the reaction as shown in Eq. 1 (molar concentration ratio of Ag^+ to HPO_4^{2-} is 3:1) (Vogel, 1990) and separately dissolved in 25 mL volumetric flask using DW. Samples were stirred, and as-resulted yellow precipitates were collected, washed several times, and dried in the oven at 105 °C for 5-10 hours. Samples were labeled as AP-0.1, AP-0.5, AP-1.0, and AP-2.0, respectively.



Photocatalytic Activity Analysis

An amount of 0.2 g of Ag_3PO_4 photocatalyst was poured into 100 mL of 10 mg/L RhB under stirring condition. Initially, the reaction was carried out under the dark condition for 20 minutes to ensure the adsorption-desorption of dye and Ag_3PO_4 photocatalyst. After that, the suspension was irradiated under blue light, and the sample was drawn ± 5 mL at a certain time. The suspension was centrifuged at 1.500 rpm, and the absorbance of the filtrate was measured (Febiyanto *et al.*, 2016).

3. RESULTS AND DISCUSSION

XRD Analysis of Ag_3PO_4 Photocatalyst

The XRD profile of as-synthesized Ag_3PO_4 was shown in Fig. 2. The diffraction of AP-0.1; AP-0.5; AP-1.0; and AP-2.0 are similar. As shown in Fig. 1, the photocatalysts synthesized under the varied concentration have a body-centered cubic of Ag_3PO_4 . It is suitable with the JCPD #06-0505 (Huang *et al.*, 2019; Yan *et al.*, 2014). High intensities of peaks and no others peak except Ag_3PO_4 , suggesting that the samples are highly crystalline and high purity (Ge, 2014).

The crystallite size of samples was calculated using the Debye-Scherrer equation as follow (Bozetine *et al.*, 2013):

$$D = \frac{K\lambda}{\beta \cos\theta} \quad (2)$$

where D , K , λ , β , and θ were crystallite size (nm), Scherrer constant (~ 0.9), a wavelength of X-ray sources (Cu $K\alpha=0.15406$ nm), FWHM (radians), and peak position (radians). Relatively, the same average diameter of crystallite was observed in all samples. Further, the ratio intensity of [110]/[200] was also investigated and summarized in Table 1.

Table 1. Crystallite size and intensity ratio calculation of Ag_3PO_4 photocatalyst samples

Samples	D_{average} (nm)	Intensity ratio of [110]/[200]
AP-0.1	52.02	0.93
AP-0.5	46.86	1.67
AP-1.0	46.96	2.02
AP-2.0	46.16	1.50

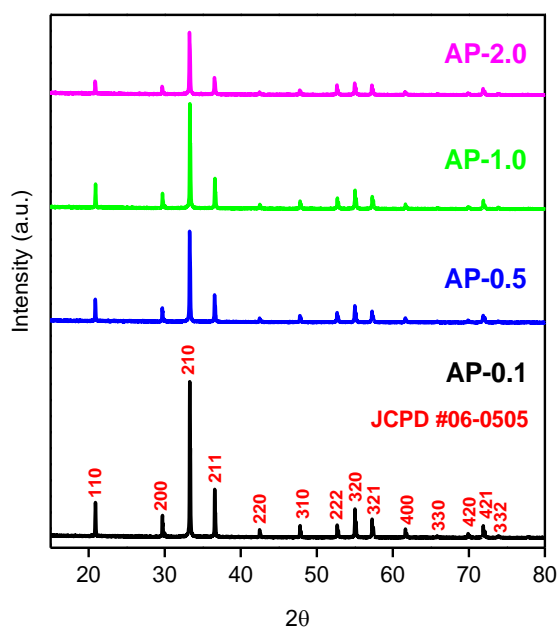


Figure 1. XRD diffraction of samples.

According to Table 1, the intensity ratio of facet planes was affected by the varied molar concentrations of reactants. The highest intensity ratio of [110]/[200] was observed in the sample of AP-1.0, suggesting that their surfaces are dominated by the [110] facet plane. This facet plane is similar to the tetrapod and rhombic dodecahedron morphology types (Martin *et al.*, 2013; Wang *et al.*, 2014). Moreover, the highest [110] dominated-facet surfaces could contribute to the improvement of the photocatalysis activity of Ag_3PO_4 photocatalyst (Bi *et al.*, 2012). Previously, the [110] facet plane of photocatalyst shows a high photocatalytic activity in the dye removal (Wang *et al.*, 2012; Zheng *et al.*, 2013).

Band gap energy analysis of Ag_3PO_4 photocatalyst

Analysis of UV-Vis absorption profiles of as-synthesized Ag_3PO_4 photocatalyst was analyzed using DRS and depicted in Fig. 2 (A-B). Based on Fig. 2 (A), samples have a good-absorption ability on the UV up to visible light (<600 nm). In addition, the difference in absorption ability could also be found in the visible wavelength at around 400-500 nm. The sample of AP-1.0 showed the highest absorption in the visible region (540-800 nm).

Fig. 2 (B) showed the band gap energy profiles of AP-0.1, AP-0.5, AP-1.0, and AP-

2.0, respectively. The band energy of samples can be estimated using the formula as follows (Eq. 3) (Rawal *et al.*, 2012):

$$\alpha h\nu = A(h\nu - E_g)^{n/2} \quad (3)$$

where α , h , ν , A , E_g , and n are absorption coefficient, Planck's constant, light frequency, a constant number, band gap energy, and value depend on the direct ($n=1$) and indirect ($n=4$) characteristics of nature semiconductor transition. According to Eq. 3, the $(\alpha h\nu)^2$ plot as a function of $h\nu$ where the band gap energy of each sample was resulted using extrapolation of a straight line towards the axis (x)-direction. The direct band gap energy of samples was summarized in Table. 2. According to Table 2, the varied molar concentrations slightly affect the light absorption as same as the band gap energy of photocatalyst samples.

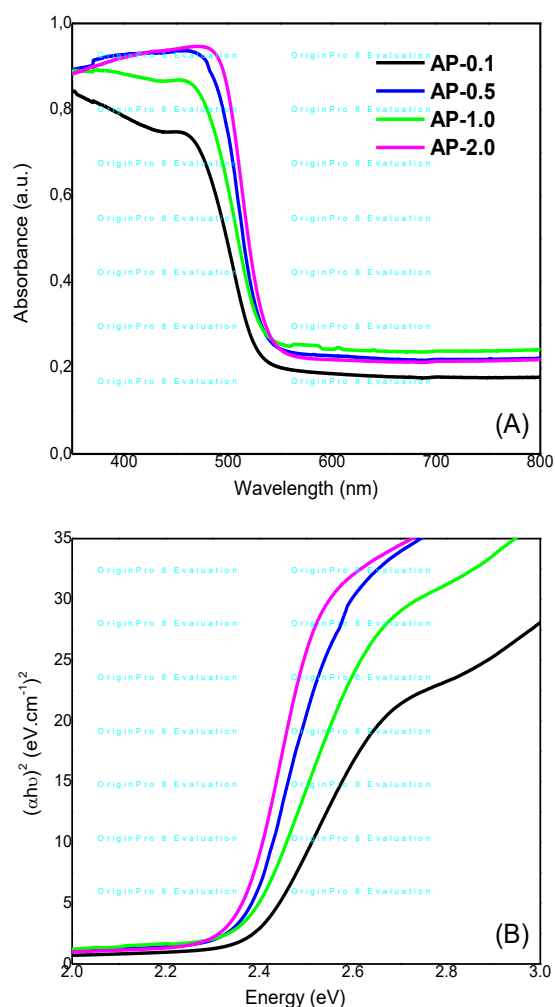


Figure 2. DRS spectra (A) and direct band gap energy characteristics (B) of samples.

Table 2. Sample characteristics of Ag₃PO₄ photocatalyst

Sampl es	Band gap energy (eV)	Linearity (R ²)
AP-0.1	2.38	0.987
AP-0.5	2.36	0.896
AP-1.0	2.36	0.960
AP-2.0	2.35	0.915

Photocatalytic activity examination of Ag₃PO₄ photocatalyst

Photocatalytic activity of as-synthesized Ag₃PO₄ photocatalyst under the varied molar concentration of reactants was performed in Fig. 3. Based on Fig. 3 (A), the control or RhB photolysis process without the addition of photocatalyst material showed a small decrease in RhB concentration under blue light irradiation. The percent RhB degradation using photolysis reaction over 80 minutes of light exposure was less than 6% (yellow color). The slight decrease in RhB photodegradation without catalyst addition could be explained by Wilhelm and Stephan (Wilhelm and Stephan, 2007) as follows: the excitation of RhB compounds (Eq. 4) is followed by O₂ reduction to be O₂^{-•} and photogenerated RhB^{+•} (Eq. 5) under the light irradiation. The O₂^{-•} radicals react with H⁺ from H₂O autoprotolysis, and then OOH[•] was resulted (Eq. 6). Subsequently, RhB cationic was degraded, resulting in CO₂, H₂O, and acid minerals (Eq. 7). Qu and Zhao reported that these reaction mechanisms are a very slow reaction, and the photocatalysis reaction using a catalyst is the best reason to explain a significant decrease in RhB photodecomposition (Qu and Zhao, 1998).



In addition, the same trends were also observed in the adsorption ability of photocatalysts under the dark condition, with a percent decrease of less than 10%, as shown in Fig. 3 (A) (green color). It concluded that RhB photodecomposition under blue light irradiation or photolysis and adsorption process at least could be neglected since there

is no apparent concentration changing compared to the RhB photodecomposition with the addition of Ag₃PO₄ photocatalyst. However, the dye photodegradation using radical species that is resulted from light-activated photocatalyst was a plausible mechanism to decrease the absorbance or dye concentration than photolysis reaction (Febiyanto *et al.*, 2019).

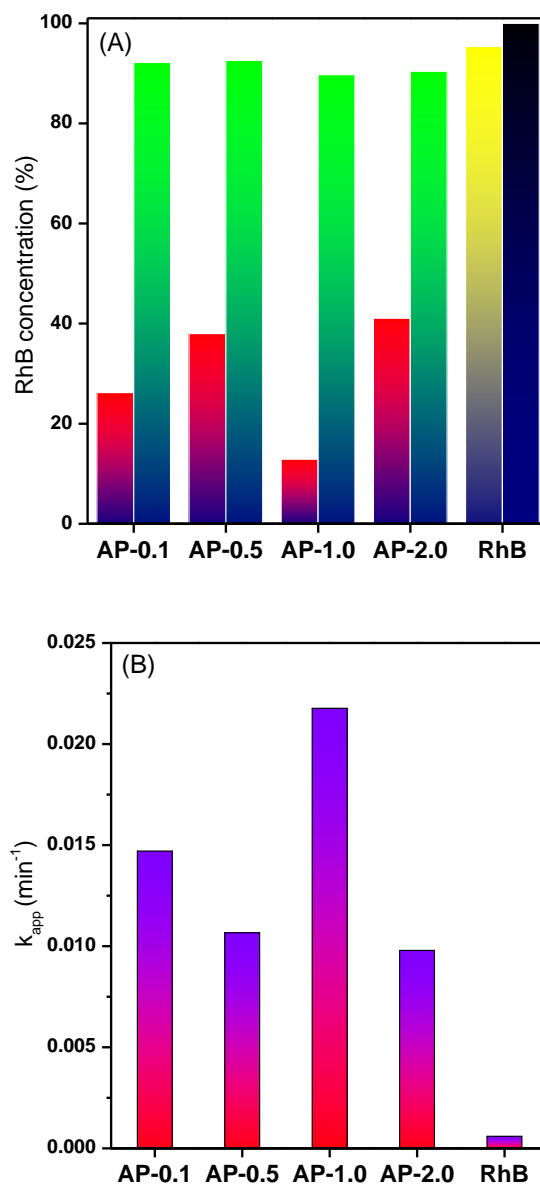


Figure 3. Photocatalytic activities of RhB over 80 minutes of light exposure under blue light (red color) and adsorption ability (green color) over 20 min in the dark condition (A), and their pseudo-first-order rate constant (B). Black and yellow colors (A) are percent initial concentration and photolysis reaction of RhB, respectively.

A significant decrease in RhB concentration was found when the RhB sample was mixed with Ag₃PO₄ photocatalyst, as shown in Fig. 3 (A). Fig. 3 (A) (red color) showed that all samples could effectively degrade the RhB dyes. The high photocatalytic activity can be found in the AP-1.0 sample, with the percent degradation of 82.5%. The high photocatalytic activity might be induced by the highest intensity of [110] facet plane and different properties obtained by co-precipitation under the starting material of AP-1.0 photocatalyst. This preparation generates high absorption along the visible region, as shown in Fig. 2 (A). The AP-1.0 is the high absorption in the visible region. This phenomenon increases the photogenerated electron and holes that lead to improving the photocatalytic activity. The percent degradation of 69.2, 57.4, and 54.3% could be observed in AP-0.1, AP-0.5, and AP-2.0, respectively. These photocatalytic activities were relatively similar and highly different from the AP-1.0 sample.

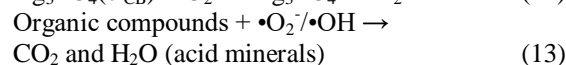
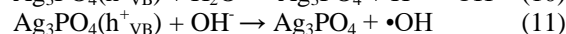
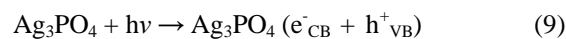
Photocatalytic kinetic analysis of Ag₃PO₄ photocatalyst with varied molar concentrations was performed in Fig. 3 (B). Rate constant can be determined from a slope that is resulted from linear regression. These can be determined using a formula as follows (Eq. 8):

$$\ln(C_o/C) = kt \quad (8)$$

where C_o , C , t , and k are initial concentration, the concentration at a certain time, irradiation time, and a rate constant of pseudo-first-order kinetic (Yan *et al.*, 2014). Based on Fig. 3 (B) and Table 2, the rate constant of samples shows a good-linearity and following the pseudo-first-order rate kinetic (Pradhan *et al.*, 2014). However, the sample with AP-1.0 showed a high photocatalytic rate kinetic of 0.0218 min⁻¹, whereas samples of AP-0.1, AP-0.5, and AP-2.0 were 0.0147, 0.0107, and 0.0098 min⁻¹, respectively. The results showed that varying molar concentrations affect the rate constant, as same as photocatalytic activities of Ag₃PO₄ photocatalyst.

The RhB oxidation and reduction mechanism chain of photocatalyst generally might be happened on the photocatalyst surfaces of Ag₃PO₄ under visible light irradiation. This following the

photodegradation mechanisms below (Guo *et al.*, 2015):



Photocatalyst under blue light excites electron (e⁻) from valence band (VB) to the conduction band (CB) resulted in electron (e⁻_{CB}) and hole (h⁺_{VB}) (Eq. 9). The electron-hole pairs transferred to the Ag₃PO₄ surfaces and oxidation/reduction of water molecules (H₂O) (Eq. 10) and OH⁻ ions or dissolved oxygen (O₂) (Eq. 11-12) can take place. Subsequently, this can produce a radical species of hydroxyl (•OH) and superoxide (•O₂⁻). The benefits of this chemical radical decompose the RhB dye structures to be small molecules such as H₂O, CO₂, and acid minerals (Eq. 13).

4. CONCLUSION

The photocatalyst of Ag₃PO₄ under the varied concentration of starting materials have been successfully synthesized using the co-precipitation method. The results showed that the varied concentrations of starting materials affect the photocatalytic activities, the intensity ratio of [110]/[200] facet plane, and their bandgap energies of Ag₃PO₄ photocatalyst. Photocatalyst synthesized using 1.0 M of AgNO₃, and 0.33 M of Na₂HPO₄·12H₂O (AP-1.0) showed the highest photocatalytic activity with the percent photodegradation of 82.5%. This is due to the high [110] facet plane and the absorption along a visible region of AP-1.0 photocatalyst. However, the [110] dominated-facet plane which is similar to the tetrapod or dodecahedron morphology structure could contribute to the improvement of photocatalysis reaction of Ag₃PO₄ photocatalyst in the RhB photodegradation.

ACKNOWLEDGMENT

This research was partly financially supported by the Directorate of Research and Community Service, Deputy of Strengthening Research and Development, Ministry of Research and Technology/National Research and Innovation Agency, Number: 176/SP2H/ADM/LT/DRPM/2020.

REFERENCES

- Afifah K, Andreas R, Hermawan D, Sulaeman U. 2019. Tuning the morphology of Ag_3PO_4 photocatalysts with an elevated concentration of KH_2PO_4 . *Bulletin of Chemical Reaction Engineering & Catalysis*. 14(3): 625–633. <https://doi.org/10.9767/bcrec.14.3.4649.625-633>
- Bi Y, Hu H, Ouyang S, Lu G, Ye J. 2012. Photocatalytic and photoelectric properties of cubic Ag_3PO_4 sub-microcrystals with sharp corners and edges. *Chem. Commun.*, 48: 3748–3750. <https://doi.org/10.1039/c2cc30363a>
- Bozetine I, Boukennous Y, Trari M, Moudir N. 2013. Synthesis and characterization of orthophosphate silver powders. *Energy Procedia*. 36: 1158–1167. <https://doi.org/10.1016/j.egypro.2013.07.131>
- Chen G, Sun M, Wei Q, Zhang Y, Zhu B, Du B. 2013. Ag_3PO_4 /graphene-oxide composite with remarkably enhanced visible-light-driven photocatalytic activity toward dyes in water. *Journal of Hazardous Materials*, 244–245: 86–93. <https://doi.org/10.1016/j.jhazmat.2012.11.032>
- Chen X, Dai Y, Guo J, Bu F, Wang X. 2016. Synthesis of micro-nano $\text{Ag}_3\text{PO}_4/\text{ZnFe}_2\text{O}_4$ with different organic additives and its enhanced photocatalytic activity under visible light irradiation. *Materials Science in Semiconductor Processing*. 41: 335–342. <https://doi.org/10.1016/j.mssp.2015.10.010>
- Dong P, Yin Y, Xu N, Guan R, Hou G, Wang Y. 2014. Facile synthesis of tetrahedral Ag_3PO_4 mesocrystals and its enhanced photocatalytic activity. *Materials Research Bulletin*. 60: 682–689. <https://doi.org/10.1016/j.materresbull.2014.09.047>
- Febiyanto, Eliani IV, Riapanitra A, Sulaeman U. 2016. Synthesis and visible light photocatalytic properties of iron oxide-silver orthophosphate composites. *AIP Conference Proceedings*. 020021: 1–7. <https://doi.org/10.1063/1.4945475>
- Febiyanto F, Soleh A, Amal MSK, Afif M, Sewiji S, Riapanita A, Sulaeman U. 2019. Facile synthesis of Ag_3PO_4 photocatalyst with varied ammonia concentration and its photocatalytic activities for dye removal. *Bulletin of Chemical Reaction Engineering & Catalysis*. 14(1): 42–50. <https://doi.org/10.9767/bcrec.14.1.2549.42-50>
- Ge M. 2014. Photodegradation of rhodamine B and methyl orange by Ag_3PO_4 catalyst under visible light irradiation. *Chinese Journal of Catalysis*. 35(8): 1410–1417. [https://doi.org/10.1016/S1872-2067\(14\)60079-6](https://doi.org/10.1016/S1872-2067(14)60079-6)
- Guo X, Chen C, Yin S, Huang L, Qin W. 2015. Controlled synthesis and photocatalytic properties of Ag_3PO_4 microcrystals. *Journal of Alloys and Compounds*. 619: 293–297. <https://doi.org/10.1016/j.jallcom.2014.09.065>
- Huang X, Gu X, Zhao Y, Qiang Y. 2019. Photoelectrochemical performance of $\text{Ag}_3\text{PO}_4/\text{Ag}$ membranes synthesized by grind coating. *Journal of Materials Science: Materials in Electronics*. 30: 19487–19492. <https://doi.org/10.1007/s10854-019-02314-9>
- Katsumata H, Taniguchi M, Kaneco S, Suzuki T. 2013. Photocatalytic degradation of bisphenol A by Ag_3PO_4 under visible light. *Catalysis Communications*. 34: 30–34. <https://doi.org/10.1016/j.catcom.2013.01.012>
- Khan A, Qamar M, Muneer M. 2012. Synthesis of highly active visible-light-driven colloidal silver orthophosphate. *Chemical Physics Letters*. 519–520: 54–58. <https://doi.org/10.1016/j.cplett.2011.11.015>
- Liu R, Hu P, Chen S. 2012. Photocatalytic activity of Ag_3PO_4 nanoparticle/ TiO_2 nanobelt heterostructures. *Applied Surface Science*. 258: 9805–9809. <https://doi.org/10.1016/j.apsusc.2012.06.033>
- Martin DJ, Umezawa N, Chen X, Ye J, Tang J. 2013. Facet engineered Ag_3PO_4 for efficient water photooxidation. *Energy & Environmental Science*. 6: 3380–3386. <https://doi.org/10.1039/c3ee42260g>
- Pradhan GK, Reddy KH, Parida KM. 2014. Facile

- fabrication of mesoporous $\alpha\text{-Fe}_2\text{O}_3/\text{SnO}_2$ nanoheterostructure for photocatalytic degradation of malachite green. *Catalysis Today*. 224: 171–179. <https://doi.org/10.1016/j.cattod.2013.10.038>
- Qu P, Zhao J. 1998. TiO_2 -assisted photodegradation of dyes: A study of two competitive primary processes in the degradation of RB in an aqueous TiO_2 colloidal solution. *Journal of Molecular Catalysis A: Chemical*. 129: 257–268.
- Rawal SB, Sung SD, Lee WI. 2012. Novel $\text{Ag}_3\text{PO}_4/\text{TiO}_2$ composites for efficient decomposition of gaseous 2-propanol under visible-light irradiation. *Catalysis Communications*. 17: 131–135. <https://doi.org/10.1016/j.catcom.2011.10.034>
- Song L, Chen Z, Li T, Zhang S. 2017. A novel Ni^{2+} -doped Ag_3PO_4 photocatalyst with high photocatalytic activity and enhancement mechanism. *Materials Chemistry and Physics*. 186: 271–279. <https://doi.org/10.1016/j.matchemphys.2016.10.053>
- Sulaeman U, Febiyanto F, Yin S, Sato T. 2016. The highly active saddle-like Ag_3PO_4 photocatalyst under visible light irradiation. *Catalysis Communication*. 85: 22–25. <https://doi.org/10.1016/j.catcom.2016.07.001>
- Vogel. 1990. *Buku Teks Analisis Anorganik Kualitatif Makro dan Semimikro*. Jakarta: PT. Kalman Media Pustaka.
- Vu TA, Dao CD, Hoang TTT, Nguyen KT, Le GH, Dang PT, Tran HTK, Nguyen TV. 2013. Highly photocatalytic activity of novel nano-sized Ag_3PO_4 for Rhodamine B degradation under visible light irradiation. *Materials Letters*. 92: 57–60. <https://doi.org/10.1016/j.matlet.2012.10.023>
- Wang B, Wang L, Hao Z, Luo Y. 2015. Study on improving visible light photocatalytic activity of Ag_3PO_4 through morphology control. *Catalysis Communications*. 58: 117–121. <https://doi.org/10.1016/j.catcom.2014.09.013>
- Wang H, He L, Wang L, Hu P, Guo L, Han X, Li J. 2012. Facile synthesis of Ag_3PO_4 tetrapod microcrystals with an increased percentage of exposed {110} facets and highly efficient photocatalytic. *CrystEngComm*. 222: 8342–8344. <https://doi.org/10.1039/c2ce26366a>
- Wang L, Li N, Zhang Q, Lou S, Zhao Y, Chen M, Teng F. 2014. An innovative glycine complexing approach to silver phosphate myriapods with improved photocatalytic activity. *CrystEngComm*. 16: 9326–9330. <https://doi.org/10.1039/C4CE01296H>
- Wilhelm P, Stephan D. 2007. Photodegradation of rhodamine B in aqueous solution. *Journal of Photochemistry and Photobiology A: Chemistry*. 185: 19–25. <https://doi.org/10.1016/j.jphotochem.2006.05.003>
- Wu A, Tian C, Chang W, Hong Y, Zhang Q, Qu Y, Fu H. 2013. Morphology-controlled synthesis of Ag_3PO_4 nano/microcrystals and their antibacterial properties. *Materials Research Bulletin*. 48(9): 3043–3048. <https://doi.org/10.1016/j.materresbull.2013.04.054>
- Xie YP, Wang GS. 2014. Visible light responsive porous lanthanum-doped Ag_3PO_4 photocatalyst with high photocatalytic water oxidation activity. *Journal of Colloid and Interface Science*. 430: 1–5. <https://doi.org/10.1016/j.jcis.2014.05.020>
- Xu YS, Zhang WD. 2013. Morphology-controlled synthesis of Ag_3PO_4 microcrystals for high performance photocatalysis. *CrystEngComm*. 15: 5407–5411. <https://doi.org/10.1039/c3ce40172c>
- Yan X, Gao Q, Qin J, Yang X, Li Y, Tang H. 2013. Morphology-controlled synthesis of Ag_3PO_4 microcubes with enhanced visible-light-driven photocatalytic activity. *Ceramics International*. 39: 9715–9720. <https://doi.org/10.1016/j.ceramint.2013.04.044>
- Yan Y, Guan H, Liu S, Jiang R. 2014. $\text{Ag}_3\text{PO}_4/\text{Fe}_2\text{O}_3$ composite photocatalysts with an n-n heterojunction semiconductor structure under visible-light irradiation. *Ceramics International*. 40: 9095–9100. <https://doi.org/10.1016/j.ceramint.2014.01.123>
- Yang Z, Tian Y, Huang G, Huang W, Liu Y, Jiao C, Wan Z, Yan X, Pan A. 2014. Novel 3D

- flower-like Ag_3PO_4 microspheres with highly enhanced visible light photocatalytic activity. *Materials Letters*. 116: 209–211. <https://doi.org/10.1016/j.matlet.2013.11.041>
- Yi Z, Ye J, Kikugawa N, Kako T, Ouyang S, Stuart-williams H, Yang H, Cao J, Luo W, Li Z, Liu Y, Withers RL. 2010. An orthophosphate semiconductor with photooxidation properties under visible-light irradiation. *Nature Materials*. 9: 559–564. <https://doi.org/10.1038/nmat2780>
- Yu H, Kang H, Jiao Z, Lü G, Bi Y. 2015. Tunable photocatalytic selectivity and stability of Ba-doped Ag_3PO_4 hollow nanosheets. *Chinese Journal of Catalysis*. 36: 1587–1595. [https://doi.org/10.1016/S1872-2067\(15\)60938-X](https://doi.org/10.1016/S1872-2067(15)60938-X)
- Zhankui C, Mengmeng S, Zhi Z, Liwei M, Wenjun F, Huimin J. 2013. Preparation and characterization of $\text{Ag}_3\text{PO}_4/\text{BiOI}$ composites with enhanced visible light driven photocatalytic performance. *Catalysis Communications*. 42: 121–124. <https://doi.org/10.1016/j.catcom.2013.08.011>
- Zheng B, Wang X, Liu C, Tan K, Xie Z, Zheng L. 2013. High-efficiently visible light-responsive photocatalysts: Ag_3PO_4 tetrahedral microcrystals with exposed {111} facets of high surface energy. *Journal of Materials Chemistry A*. 1: 12635–12640. <https://doi.org/10.1039/c3ta12946b>